Clays and Clay Minerals, Vol. 62, No. 5, 415–424, 2014.

DYNAMIC ADSORPTION OF Cd^{2+} ONTO ACID-MODIFIED ATTAPULGITE FROM AQUEOUS SOLUTION

Na Guo[1,2], Jin-Sheng Wang[1,2,*], Jian Li[1,2], Yan-Guo Teng[1,2], and Yuan-Zheng Zhai[1,2]

[1] College of Water Sciences, Beijing Normal University, Beijing100875, China
[2] Engineering Research Center of Groundwater Pollution Control and Remediation, Ministry of Education of China, Beijing100875, China

Abstract—In the present study, acid-modified attapulgite was used, as an adsorbent, to remove as much Cd^{2+} as possible from aqueous solution. Static adsorption experiments using powdered acid-modified attapulgite, and dynamic adsorption using granular acid-modifed attapulgite, were conducted to explore the practical application of modified attapulgite in the adsorption of Cd^{2+}. The modified attapulgite had a larger specific surface area and thinner fibrous crystals than the unmodified version. No obvious differences were noted, in terms of the crystal structure, between the natural attapulgite and the modified version. The effects of initial concentration, pH, contact time, and ionic strength on the adsorption of Cd^{2+} were investigated, and the results showed that the adsorption capacity of the modified attapulgite was increased with increasing pH and the initial Cd^{2+} concentration. The adsorption properties were analyzed by means of dynamic adsorption tests with respect to various Cd^{2+} concentrations and flow rates. The maximum adsorption capacity of 8.83 mg/g occurred at a flow rate of 1 mL/min and at an initial concentration of 75 mg/L. Because there was better accord between the data and a pseudo-second order model than a pseudo-first-order model, external mass transfer is suggested to be the rate-controlling process. The experimental data were also fitted for the intraparticle diffusion model, implying that the intraparticle diffusion of Cd^{2+} onto the modified attapulgite was also important for controlling the adsorption process. The Bohart-Adams model was more suitable than the Thomas model for describing the dynamic behavior with respect to the flow rate and the initial Cd^{2+} concentration. This research provided the theoretical basis for the dynamic adsorption of Cd^{2+} on the modified attapulgite. Compared to the powdered modified attapulgite, the dynamic adsorption by granular modified attapulgite appeared more favorable in terms of practical application.

Key Words—Breakthrough Curve, Cd^{2+}, Dynamic Adsorption, Modified Attapulgite.

INTRODUCTION

The increasing level of toxic metals discharged to the environment as industrial wastes represents a serious threat to human health, living resources, and ecological systems. Among these heavy-metal ions, Cd^{2+} is a non-essential and highly toxic heavy-metal element that can be released into the environment by various means (Huang *et al*., 2011). The treatment of Cd^{2+}-contaminated waste water prior to discharge is essential (Salehi *et al*., 2012) in terms of environmental protection. In recent years, techniques for the removal of heavy metals from effluents have mainly included chemical oxidation, precipitation, electrochemical extraction, evaporation, and ion-exchange (Ngah and Fatinathan, 2008). The adsorption technique has significant potential because of its convenience and renewability (Cao *et al*., 2012). Research into the production of alternative adsorbents to reduce the cost of waste-water treatment has intensified in recent years. Clay minerals are now used widely in the removal of heavy-metal ions, dyes, and other organics from aqueous solution because of their large surface area, low cost, ready availability, and environmental stability (Falayi and Ntuli, 2013). The removal of Pb^{2+} by bentonite was investigated by Inglezakis *et al*. (2007) who found that the removal of Pb^{2+} reached 100% at ambient temperature and mild agitation (100 rpm). The novel chitosan-*g*-poly-attapulgite composites were applied (Wang *etal*., 2009) as adsorbents in the removal of Cu^{2+} from aqueous solution, and >90% of the adsorption occurred within the initial 15 min. Clay minerals clearly have potential for the removal of metal ions from aqueous solution (John, 1972; Aly and Koji, 1981).

Attapulgite (AT) is a hydrated magnesium aluminum silicate present in nature as a fibrous clay mineral containing ribbons of a 2:1 structure (Haden and Schwint, 1967). Numerous studies have been carried out on the adsorption of toxic metals, and inorganic and organic pollutants, from aqueous solution by natural or modified AT (Akyuz *et al.*, 1994; Saglam *et al*., 2000). Acid activation is a widely used treatment for improving the adsorption properties of AT (Suárez Barrios *et al.*, 1995) which can increase the surface area by dissolving impurities. Many Si-OH groups on the surface of AT can be obtained by acid activation, influencing the adsorption capacity, and the adsorption mechanism of heavy metals on AT (Frini-Srasra and Srasra, 2010).

* E-mail address of corresponding author:
602284777@qq.com
DOI: 10.1346/CCMN.2014.0620505

https://doi.org/10.1346/CCMN.2014.0620505 Published online by Cambridge University Press

For Cd^{2+} adsorption, experimental results have shown that the adsorption capacity of Cd^{2+} was 6.07−13.15 mg/g after 90 min (Fan *et al*., 2009). According to Wang and Wang (2010), >90% of Cd^{2+} adsorption on hydrogel-modified AT occurred within the first 3 min and adsorption equilibrium was reached within 10 min. Various materials have been reported in the literature as being effective at the removal of Cd^{2+}, but these cannot be applied in practice because of the difficulty of separating powdered materials from waste water for regeneration. Many differences, in terms of adsorption performance, exist between powdered and granular materials, and their adsorption capacities vary significantly (Liu and Liu, 2014). In addition, previous studies of the adsorption of Cd^{2+} on AT were mainly batch experiments which provided certain preliminary information such as optimum pH, approximate time for adsorption, and the adsorption capacity of the adsorbent. These data were less suitable for use at an industrial scale where large quantities of waste water were being generated on an ongoing basis. The dynamic adsorption mechanism has rarely been reported, limiting potential practical application of this phenomenon.

The objective of the present study was to provide the required basis for the design and fabrication of practical adsorption systems by analyzing the static adsorption process of the powdered acid-modified attapulgite (A-AT) and the dynamic adsorption characteristics of granular A-AT. Static adsorption experiments used powdered AT and A-AT to determine the adsorption properties and the effects of a number of variables. The data from the static experiments were used to constrain dynamic adsorption experiments using granular A-AT designed to study the potential practical application. The effects of various variables, such as initial Cd^{2+} concentration, flow rate of the fluid, pH, contact time, and ionic strength were studied using the powdered A-AT to determine the optimum conditions for adsorption. The performance of the adsorbent in the dynamic adsorption was described by the shape of the 'breakthrough curve,' and the adsorption mechanism was inferred by analyzing the variation of the model parameters.

MATERIALS AND METHODS

Reagents

The attapulgite used here was from Xuyi, Jiangsu Province, PR China, and had two particle sizes: 3.0 mm and 200 British Standard Sieve (BSS) mesh (75 μm) (Xuyi Huahong Mining Co., Ltd, Xuyi, China). The Cd^{2+} stock solution, 1 g/L, was prepared by dissolving 0.50 g of Cd (Sinopharm Chemical Reagent Co., Ltd, Beijing, China) in 10 mL of 5 mol/L HNO_3 (Xilong Chemical Co., Ltd, Shantou, China) and diluting to 1000 mL. Hydrochloric acid (HCl, 36−38%), sodium hydroxide (NaOH), and potassium borohydride (KBH_4, >98%) were of analytical reagent grade (Sinopharm Chemical Reagent Co., Ltd, Beijing, China). All the solutions were prepared using high-purity water (Beijing Jiulu water station, Beijing, China).

Adsorbent

Following the approach of Qi *et al*. (2007) the AT was added to 4% (w/v) HCl in a ratio (v/w) of 5:1 (HCl/attapulgite) to exchange the interlayer cations with H^+ and to dissolve the impurities such as dolomite and calcite in the pores of AT. The mixture was stirred for 30 min under magnetic stirring (H01-1B, Shanghai Mei Yingpu Instrument Manufacturing Co., Ltd, Shanghai, China) and dispersed in an ultrasonic bath (KQ-250DB, Kun Shan Ultrasonic Instruments Co., Ltd, Kunshan, China) for 1 h at 25ºC. The precipitate was separated by centrifuging at $974 \times g$ for 15 min (Biofuge primo R, Thermo Sorvall, Shanghai, China) and washed repeatedly to remove the water-soluble particles and then filtered. The A-AT was aged for 2 h at 70ºC and then dried, crushed, and sieved to the particle size of a 100-mesh screen (150 μm); then the granular A-AT was achieved by the granulation of AT.

Experimental studies

The influences of various physico-chemical factors such as pH, initial Cd^{2+} concentration, and contact time, as considered in previous studies (Zou *et al*., 2011; Wu and Zheng, 2013), were selected for study here in batch-adsorption experiments using the powdered A-AT. The experiments were conducted in 50 mL Erlenmeyer flasks with 20 mL of Cd^{2+} solution at different concentrations, varying from 50.0 to 100.0 mg/L. The samples were shaken mechanically at 25ºC for 72 h on a rotating shaker (ZHWY-100D/103D, Zhcheng, Shanghai, China). The supernatant solution was then centrifuged at $1431 \times g$ for 15 min, and the concentration of Cd^{2+} was monitored using an AFS-230E dual-channel atomic fluorescence spectrophotometer (Beijing Kechuang Haiguang Instrument Co., Ltd, Beijing, PR China) at the high voltage of 250 eV and the peak current of 40 mA.

The dynamic adsorption procedure was conducted to measure the equilibrium adsorption capacity of A-AT, and the effects of the physico-chemical parameters such as flow rate and initial Cd^{2+}concentration, were determined. In the column experiment, 25.0 g of granular A-AT was placed in a polytetrafluoroethylene (PTFE) column (10.0 cm × 3.0 cm) using the slurry method, and the bed thickness of the A-AT was 5.00 cm. The column was loaded with the Cd^{2+} solution which percolated upward at a concentrantion ranging from 50 to 100 mg/L at ambient temperature and the flow rate of 1.0 mL/min. The effect of the flow rate was determined by varying from 0.5 to 2.0 mL/min at the concentration of 75 mg/L. The column operation was terminated when 95% of the adsorption capacity was exhausted.

https://doi.org/10.1346/CCMN.2014.0620505 Published online by Cambridge University Press

Characterization and instrumentation

Ultrathin sections of AT and A-AT were obtained for studies of the morphology by means of transmission electron microscopy (TEM) using a Tecnai G2 20 (FEI Company, USA). Full structural characterizations of the AT and A-AT were performed using Fourier-transform infrared (FTIR) spectroscopy (Nexus 670, Nicolet, USA) and X-ray diffraction (XRD) (X'Pert PRO MPD, PANalytical B.V., The Netherlands). The specific surface areas of AT and A-AT were evaluated by measuring N_2 isotherms at 77 K (Quantachrome v3.0, Quantachrome Company, USA). The Cd^{2+} concentration was determined using a dual-channel atomic fluorescence spectrophotometer (AFS-230E, Beijing Kechuang Haiguang Instrument Co. Ltd, China) at 250 eV and 40 mA.

RESULTS AND DISCUSSION

Effect of acid modification on AT

Lattice spacings for AT and A-AT were calculated from XRD reflections (not shown here) using the Bragg formula, yielding d_{200} of 0.638 nm and 0.652 nm, respectively. The similarity indicated that the acid-modification treatment of AT had no obvious effect on its crystal structure, consistent with the previous studies (Peng *et al*., 2004; Chen, Z.G. *et al*., 2010). The small difference between them suggests that the modification method did not change the crystal lattice spacing and affected only the surface of the AT. In order to study the surface alterations, the specific surface areas of AT and A-AT were measured by the nitrogen adsorption method. The result showed that the specific surface area of A-AT (97 m^2/g) was more than four times that of AT (24 m^2/g).

Morphological images of the AT and A-AT (not shown) revealed that AT has a fibrous morphology in which the straight fibers were oriented randomly, similar to the fibrous texture described in previous studies (Xi *et al*., 2010; Aiban, 2006). The fibers were ~200–250 nm long and ~15–20 nm wide. Compared to AT, A-AT in water stirred mechanically with the aid of an ultrasonic wave was arranged more regularly, but very few single fibrous crystals were found due to the strong interaction between the fibrous crystals. The A-AT was better dispersed, and consisted of thinner fibers than AT (Xi *et al*., 2010), and was therefore more suitable for prilling (making into pellets).

The FTIR spectra of AT and A-AT (Figure 1) showed no difference in terms of the characteristic bands and their locations. In the high-frequency region (1700–4000 cm^{-1}), the 3401 cm^{-1} and 3552 cm^{-1} band (-OH) and the band at ~3616 cm^{-1} (Al-OH) were found. In the intermediate frequency region (800–1700 cm^{-1}), the 986 cm^{-1} and 1027 cm^{-1} bands were the main characteristics representing the stretching vibration ranges of (Mg, Al)–Si–O and Si–O–Si, respectively. In the low-frequency range (400–800 cm^{-1}), the 796 cm^{-1} band belongs to the characteristic peak of free silica, indicating that the AT had impurities not completely removed during modification.

Adsorption kinetics studies

The adsorption of Cd^{2+} onto A-AT as a function of contact time and initial concentration at solution pH 7.0 (Figure 2) indicated that with the increase in initial Cd^{2+} concentration from 50 to 100 mg/L, the amount of Cd^{2+} adsorbed by A-AT increased from 9.799 to 19.330 mg/g and the removal ratios all reached >90%. At low concentrations (1 mg/L, 5 mg/L, and 10 mg/L), the removal ratios reached 100% at 6 h, 6 h, and 18 h, respectively. At the fixed concentration of 50 mg/L, the adsorption capacity of the A-AT was 25% greater than that of the AT. Furthermore, the adsorption capacity of Cd^{2+} on A-AT was >1 order of magnitude greater than that of Cd^{2+} on the hyper-branched aliphatic polyester-grafted AT and the aminopropyl AT (Liu and Wang, 2007). Adsorption kinetics experiments revealed three

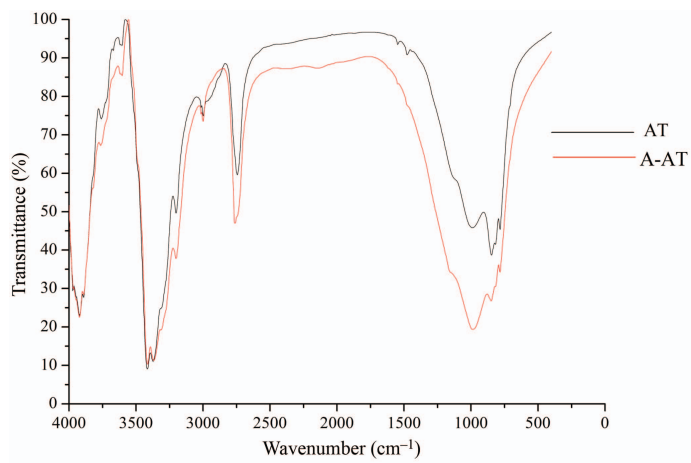


Figure 1. FTIR spectra of AT (upper trace) and A-AT (lower trace).

https://doi.org/10.1346/CCMN.2014.0620505 Published online by Cambridge University Press

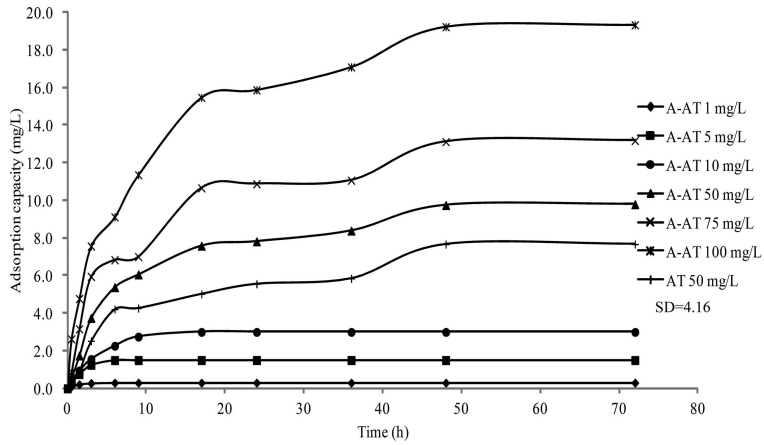


Figure 2. Effect of contact time on Cd^{2+} adsorption onto AT and A-AT at different concentrations.

stages in the adsorption process (Figure 2), in agreement with previous reports (Chen and Wang, 2009). The amount adsorbed increased rapidly during the initial adsorption stage and then continued to increase slowly with contact time. When it reached the equilibrium point, the adsorption stopped. Half (50%) of the adsorption took place within the first 3 h.

To provide better insight into the adsorption mechanism of Cd^{2+} onto A-AT, the experimental data were described by pseudo-first-order and pseudo-second order kinetic models. The pseudo-first order Lagergren model was generally formulated as follows (Zou *et al*., 2011):

$$\ln(q - q_t) = \ln(q) - k_1 t \quad (1)$$

and the pseudo-second order model was represented as (Wang *et al*., 2006):

$$\frac{t}{q_t} = \frac{1}{k_2 q^2} + \frac{t}{q} \quad (2)$$

where q_t and q are the adsorption at time t and at equilibrium, respectively. k_1 and k_2 are rate constants of the pseudo-first order and pseudo-second order models, respectively.

The rate constants k_1 and k_2 and the equilibrium adsorption capacity, q, with correlation coefficients R for the pseudo-first order and pseudo-second order models were calculated (Table 1). The results indicated that with increasing concentration from 50 to 100 mg/L at 25ºC, the pseudo-first order rate constant, k_1, increased from 0.054 to 0.102/min, and the pseudo-second order rate constant, k_2, decreased from 0.012 to 0.008 g/(mg·min). The correlation coefficients for the pseudo-second order kinetic model were much greater than the pseudo-first order kinetic model, in the range 0.993–0.996, confirming very good agreement with the experimental data. The decrease in k_2 indicated that the adsorption of Cd^{2+} reached equilibrium more quickly at a lower initial concentration. The value of the equilibrium adsorption capacity was 14.306 mg/g, close to the value of capacity (13.178 mg/g) for an initial Cd^{2+} concentration of 75 mg/L. When the initial Cd^{2+} concentration increased from 50 to 75 mg/L, the equilibrium concentration, q_e, increased rapidly, whereas it increased slowly with an initial concentration of up to 100 mg/L. A similar phenomenon was observed in the adsorption of Congo red dye by Ca-bentonite (Lian *et al*., 2009).

The intraparticle diffusion model may be used to determine the effect of diffusion resistance in the adsorption mechanism. This model was represented by the following equation (Chen, J.H. *et al*., 2010):

$$q_t = k_p\sqrt{t} + c \quad (3)$$

where k_p is the rate constant of the model. The correlation coefficients (R^2) for the intraparticle diffusion model were

Table 1. Comparison of the different kinetic model parameters at 25ºC.

C_0 (mg/L)	q_e (mg/g)	Pseudo-first order kinetic model			Pseudo-second order kinetic model			Intraparticle diffusion model		
		R_1	q_1	k_1	R_2	q_2	k_2	R_3	c	k_p
50	9.789	0.955	7.626	0.054	0.995	10.799	0.012	0.963	0.663	1.429
75	13.178	0.980	13.371	0.104	0.993	14.306	0.010	0.962	1.128	1.876
100	19.330	0.982	14.571	0.102	0.996	20.833	0.008	0.977	1.712	2.768

https://doi.org/10.1346/CCMN.2014.0620505 Published online by Cambridge University Press

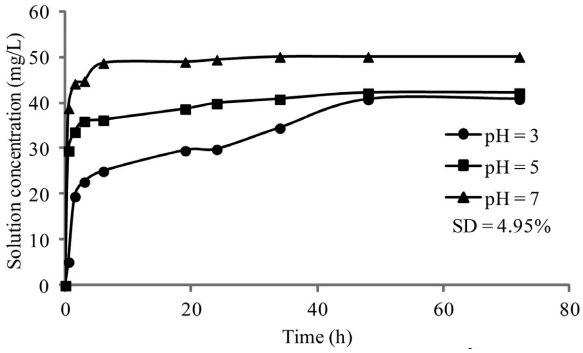


Figure 3. Effect of initial pH on the adsorption of Cd^{2+}onto A-AT.

between 0.962 and 0.977, indicating that the adsorption of Cd^{2+} onto A-AT may be described by the intraparticle diffusion model. External mass transfer was the main mechanism during the initial period, followed by the intraparticle diffusion mechanism of Cd^{2+} onto A-AT.

Evaluation of different parameters

pH effect on the sorption of Cd^{2+}. To better understand the adsorption mechanism, the effect of pH on the adsorption of Cd^{2+} to A-AT was examined within the pH range 3−7. As the pH values of the experiments reported here were ⩽7, the coprecipitation of Cd^{2+} ions as $Cd(OH)_2$ which occurs simultaneously at pH > 7, and could lead to an inaccurate interpretation of the adsorption (Alvarez *et al*., 2012), did not affect the results presented here. In the present study, the sorption of Cd^{2+} on the sorbent was conducted at a fixed concentration of 50 mg/L, and the results (Figure 3) demonstrated that the adsorption capacities increased with increase in pH. Compared to the adsorption process at pH 3 and 5, the process at pH 7 was faster, and 77.4% of the adsorption occurred within 60 min. Adsorption equilibrium was achieved after ~6 h, and the maximum adsorption capacity was 20.0 mg/g. The amount adsorbed and the characteristics of the adsorption process were very dependent on the initial pH of the solution. This finding was in agreement with recent works by other authors (Guerra *et al*., 2010) who found the same behavior by studying the adsorption capacity of uranyl onto modified AT.

Metal-ion adsorption is due to electrostatic interaction between metal ions and the negatively charged surface of the adsorbent (Zou *et al*., 2011). This can be explained by the competitive adsorption between hydrogen ions and target ions for the same active adsorption site in the absence of interfering competitive ions, as reported in the literature (He *et al*., 2008). As the value of pH increased, the adsorption surface became less positive due to the decrease in competition for the adsorption sites; therefore, electrostatic attraction and ion-exchange between the metal ions and the surface of the attapulgite were likely to be increased.

Effects of the ionic strength. To examine the effect of the ionic strength on the uptake of Cd^{2+} by the adsorbent at fixed pH value, the adsorption of Cd^{2+}on A-AT was also studied in the presence of electrolytes such as NaCl, KCl, and $AlCl_3$. The results (Figure 4) showed that the adsorption of Cd^{2+} was greatest (7.635 mg/g) in 0.01 mol/L NaCl solution and smallest (5.501 mg/g) in 0.1 mol/L LiCl solution at pH = 3, indicating that the cationic competitive adsorption existed on the surface of A-AT and influenced the adsorption of Cd^{2+}. The slight decrease in the Cd^{2+} adsorption capacity after an increase in ionic strength of Na^+ from 0.01 to 0.1 mol/L indicated that electrostatic attraction was the main adsorption mechanism, and the ionic strength should have a significantly negative effect on the adsorption process, in accord with previous studies (Ding and Shang, 2010; Lin *et al*., 2011). Comparing the adsorption capacities of 0.1 mol/L Li^+, Na^+, and K^+ in the present study, the adsorption capacity for 0.1 mol/L K^+ (7.403 mg/g) was greater than that of 0.1 mol/L Na^+ (6.356 mg/g) and 0.1 mol/L Li^+

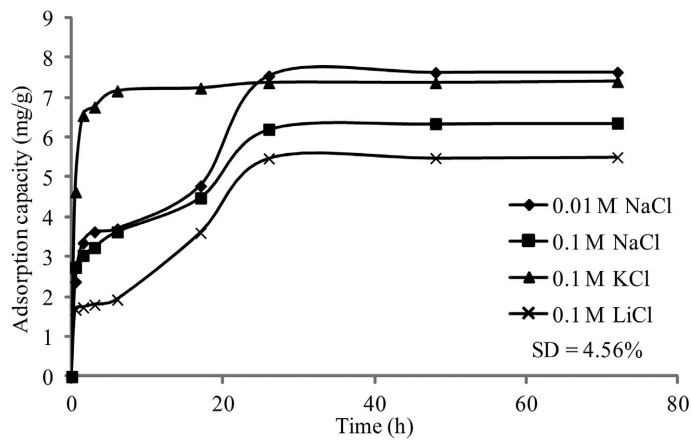


Figure 4. Effect of ionic strength on the adsorption of Cd^{2+}on A-AT at pH = 3 and m/V = 50 mg/L.

https://doi.org/10.1346/CCMN.2014.0620505 Published online by Cambridge University Press

(5.501 mg/g), due to the smaller radius of Li^+ compared to Na^+ and K^+. Li^+ had the highest affinity for the A-AT surface and the greatest tendency for counter-ion exchange with the surface groups of the adsorbent, in agreement with previous studies (*e.g.* Ma *et al*., 2011). The relative influences of foreign metal ions on the adsorption of Cd^{2+} to A-AT at pH = 3 was $Li^+ > Na^+ > K^+$.

The adsorption of Cd^{2+} to A-AT was influenced by the foreign ions during the initial phase of the adsorption process; the adsorption capacities did not make a difference. The results indicated that the influence of the ionic strength on the adsorption of metal ions was dominant, and the adsorption mechanism of ion exchange was ionic strength-dependent (Pehlivan *et al*., 2008). This confirmed that the ionic strength was the main controlling factor at the initial stage of the adsorption process, and gradually, other mechanisms such as hydrogen bonding and surface complexation controlled the adsorption process so that ionic strength had a slightly negative effect on the adsorption capacity.

Dynamic sorption studies

Effect of the flow rate. To study the effect of the flow rate through the bed thickness, the flow rate was varied from 1.0 to 2.0 mL/min at the inlet concentration of 75 mg/L. The breakthrough curve point was the point where the concentration of the effluent from the adsorption column exceeded the standard or was related to a particular value (Pokhrel and Viraraghavan, 2008; Pan *et al*., 2005). In the dynamic adsorption experiments, the breakthrough curve point of the dynamic adsorption experiments was set to 15% (C_t/C_0 = 0.15, C_0 was the initial adsorption concentration (mg/L) and C_t was the concentration of the effluent at adsorption time t (mg/L)). The breakthrough curves (Figure 5) showed that the uptake of Cd^{2+} onto A-AT and the breakthrough time decreased with increase of the flow rate. Furthermore, the breakthrough curve became steeper at the initial stage of adsorption with increase in the flow rate. This can be explained by the fact that the adsorption of Cd^{2+} by A-AT was affected by the insufficient residence time of the solute in the column, which controlled the diffusion of the solute into the pore space of the adsorbent and the contact between Cd^{2+} and the active sites. In other words, the residence time of the solute in the column was insufficient to reach adsorption equilibrium at the given flow rate. The results were also in agreement with those referred to above (Hasan *et al*., 2010; Bhargavi *et al*., 2013).

The dynamic sorption data were evaluated, and the saturated adsorption capacities were compared (Table 2). When the flow rate was increased from 1.0 to 2.0 mL/min, the adsorption capacity decreased from 8.83 to 6.08 mg/g. The volume of the effluent treated up to the breakthrough concentration decreased rapidly from 1316 mL to 16 mL with the increase in flow rate.

Effect of the initial concentration. The adsorption performance of A-AT was tested at various Cd^{2+} inlet concentrations. The breakthrough curves (Figure 6) were obtained by changing the initial concentration from 50 to 100 mg/L at a flow rate of 1 mL/min. The volume treated before the A-AT bed became saturated and the breakthrough time decreased with increase in the initial concentration. As expected, a high inlet concentration may saturate the adsorbent more quickly. The adsorption capacity did not vary monotonically with the inlet concentration varying from 50 to 100 mg/L (Uddin *et al*., 2009), and the largest adsorption capacity (8.83 mg/g) occurred at the inlet concentration of 75 mg/L.

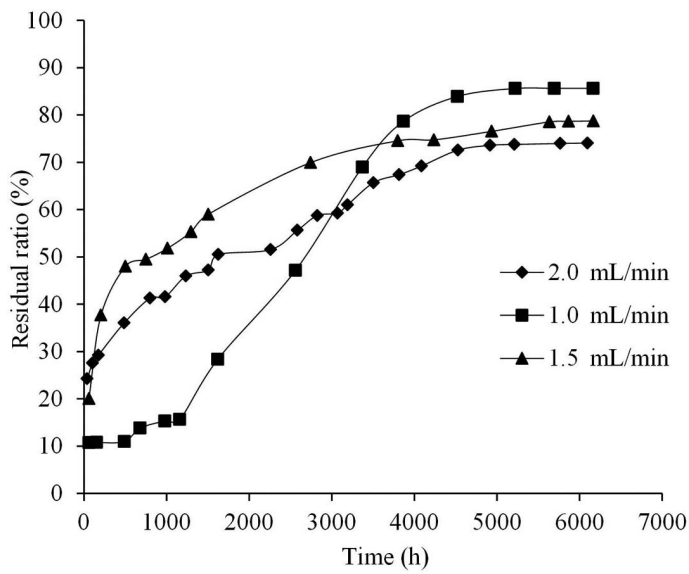


Figure 5. Effect of flow rate on the breakthrough curves of Cd^{2+}.

https://doi.org/10.1346/CCMN.2014.0620505 Published online by Cambridge University Press

Table 2. Constants of the Thomas and Bohart-Adams models for the adsorption of Cd^{2+} onto A-ATP.

Item	c_0 (mg/L)	Q (mL/min)	x (cm)	m (g)	N_0 (mg/g)	t $C_t/C_0 = 20\%$ (min)	Thomas model K_{Th} (mL/(min·mg))	q_0 (mg/g)	R	SSE	Bohart-Adams model a (min/min)	b (min)	k (L/min/mg)	R	SSE
Concentration variation	50	1.0	10	25.05	6.24	2241	0.00003	5.241	0.962	12.742	44.82	1792.80	−0.00021	0.997	8.371
	75	1.0	10	25.05	8.83	1316	0.00001	8.912	0.978	16.861	17.55	1140.53	−0.00002	0.985	14.251
	100	1.0	10	25.05	5.23	72	0.000004	8.391	0.956	24.529	0.72	64.80	−0.00002	0.992	13.362
Velocity variation	75	1.0	10	25.05	8.83	1316	0.00001	8.912	0.978	16.861	17.55	1140.53	−0.00124	0.985	14.251
	75	1.5	10	25.05	6.39	39	0.000009	8.620	0.963	15.046	0.35	35.53	−0.00052	0.981	15.274
	75	2.0	10	25.05	6.08	16	0.000006	4.998	0.968	15.772	0.11	14.93	−0.00002	0.979	16.310

Q: linear flow rate
SSE: sum of squares for error

All the results demonstrated that the change in the concentration gradient affected the saturation rate and the breakthrough time, which was the driving force for adsorption. A high concentration gradient provided a strong driving force for the adsorption process, explaining why the adsorption capacity increased when the inlet concentration changed from 50 to 75 mg/L. As the concentration increased further, the limited number of active sites was insufficient to absorb Cd^{2+} in the solution, and an excess of Cd^{2+} may even block the pores of the adsorbent to affect the adsorption capacity, explaining why the adsorption capacity was least (5.23 mg/g) at the inlet concentration of 100 mg/L.

Modeling of the dynamic study results. The dynamic adsorption data obtained from the column experiments were described by the Bohart-Adams model (Bhargavi *et al*., 2013) and the Thomas model (Xiao *et al*., 2009). The Bohart-Adams model is based on surface-reaction theory, and it assumes that equilibrium is not instantaneous.

$$\text{Thomas: } \ln\left(\frac{C_0}{C_t} - 1\right) = \frac{K_{Th} q_0 m}{Q} - K_{Th} C_0 t_e \quad (4)$$

$$\text{Bohart-Adams: } t = \frac{q_0 x}{C_0 v} - \ln\left[\frac{C_0}{C_b} - 1\right] \times \frac{1}{C_0 K} \quad (5)$$

A simplified form of the Bohart-Adams model is as follows:

$$t = aX + b \quad (6)$$

where $a = \frac{N_0}{C_0 v}$ and $b = \ln(\frac{C_0}{C_b} - 1) \times \frac{1}{C_0 K}$. t is the time to the breakpoint (h); C_0 is the influent concentration (mg/L); C_b (mg/L)and t_e (min) are the concentration and the time at breakthrough, respectively; N_0 is the adsorption capacity of the adsorbent (mg/g); x is the bed thickness of the column (cm); v and Q are the linear flow rate (mL/min); K and K_{Th} are the rate constants (L/mg·h); q_0 is the equilibrium adsorbate uptake (mg); and m is the mass of the adsorbent in the column (mg).

The Bohart-Adams model is based on the surface reaction theory (Chowdhury *et al*., 2013) and assumes that equilibrium is not instantaneous, and that the rate of sorption is proportional to the fraction of sorption capacity still remaining on the adsorbent. The derivation of the Thomas model is based on second-order reaction kinetics, and it assumes no axial dispersion is associated with the adsorption (Aksu and Gönen, 2004). The Thomas model is suitable for describing the adsorption process without external and internal diffusion limitations (Singh *et al*., 2011).The Bohart-Adams model can be considered as a simple form of the Thomas model when the isotherm is highly favorable. The difference between the models is in the adsorption kinetics, where the Thomas model considers that the description of adsorption has been in accordance with the principle of the second-order reversible reaction (Borba *et al*., 2008).

https://doi.org/10.1346/CCMN.2014.0620505 Published online by Cambridge University Press

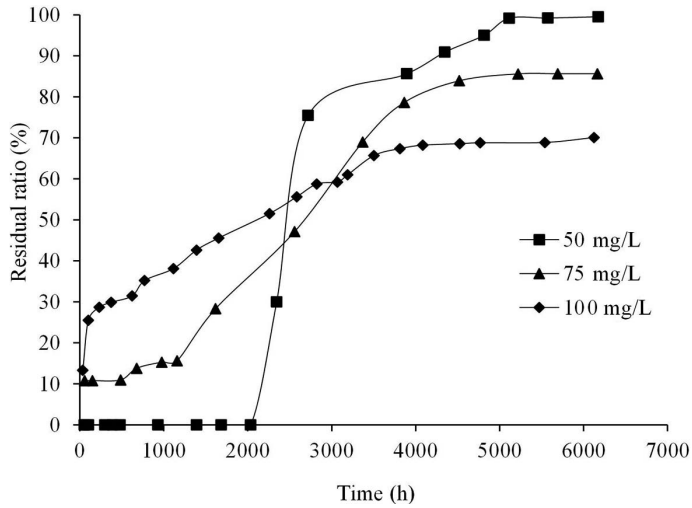


Figure 6. Effect of initial concentration on the breakthrough curves of Cd^{2+}.

The correlation coefficients (R) of the Bohart-Adams model (0.979–0.997) and the Thomas model (0.956–0.978) were all above the confidence level of 95% (0.707) at $n = 8$. The better values of the correlation coefficient in the Bohart-Adams model showed that the variation of the concentration and the velocity with the adsorption capacity was more highly linear than those in the Thomas model, indicating the validity of the Bohart-Adams model when applied to continuous column studies. Although the Thomas model gave a poor fit of the experimental data at higher concentrations, a superior agreement between the experimental and the predicted normalized concentration values was achieved at all flow rates and low concentrations. This was because the Thomas model was more suitable for adsorption processes where the external and internal diffusion was not the limiting step, and the latter became more important with the increase in concentration. The K_{Th} coefficient of the Thomas model decreased from 0.00003 to 0.000004 mL/min·mg with the increase in inlet concentration, demonstrating that the adsorption capacity can be explained on the basis of mass-transfer fundamentals, and the molecular diffusion occurring in the solid–liquid interface was the key factor. The rate constants of the Bohart-Adams model were also influenced by the flow rates and had a tendency to increase with the increase in flow rate, indicating that the overall system kinetics was dominated by the external mass transfer in the initial part of the sorption in the column (Hasan *et al*., 2010).

The model parameters calculated indicated that the linear regression equation and the experimental equations did not match perfectly in the second stage of the adsorption process. This can be explained as follows. On the one hand, the Thomas model and the Bohart-Adams model were both considered to follow these assumptions: (1) the adsorption is described by a pseudo-second order reaction rate principle which reduces to a Langmuir isotherm at equilibrium; (2) the intraparticle diffusion and the external resistance during the mass-transfer processes are considered to be negligible; and (3) isothermal and isobaric process conditions (Bohart and Adams, 1920; Thomas, 1944). The adsorption of Cd^{2+} on A-AT was not only limited by the surface adsorption but also controlled by the interphase mass transfer. On the other hand, this deviation may be found in hydrodynamic phenomena, *e.g.* axial dispersion, and related to the velocity gradients in the column (Borba *et al*., 2008).

Comparison of batch and dynamic experiments

The sorption distribution coefficients (K_d) at different initial Cd^{2+} concentrations in static and dynamic experiments were calculated by equations 7 and 8, respectively.

$$K_d = \frac{C_0 - C_{eq}}{C_{eq}} \times \frac{V}{G} \quad (7)$$

where K_d is the sorption distribution coefficient; C_0 (mg/L) and C_{eq} (mg/L) are the initial concentration and the adsorption equilibrium concentration, respectively; V is the volume of the solution; and G is the quantity of the absorbent. The quantity of absorbent was weighed by electronic scales in the static experiments.

$$K_d = S/W \quad (8)$$

where S (mg) and W (mg) are the amounts of solute in the solid phase and the liquid phase at equilibrium, respectively.

A large difference was found between the sorption distribution coefficients obtained by the batch and the dynamic experiments (Table 3), suggesting that the particle size and the level of mixing could be possible

https://doi.org/10.1346/CCMN.2014.0620505 Published online by Cambridge University Press

Table 3. Sorption distribution coefficients of the static and dynamic experiments.

C_0 (mg/L)	Static experiment	Dynamic experiment
50	9.30	1.57
75	1.45	1.29
100	5.77	0.47

causes of this discrepancy. In the batch experiment, the solution was mixed more thoroughly with the adsorbent, so the larger K_d value was obtained more easily, in accordance with a previous study (Zhang *et al*., 2012).

CONCLUSIONS

The present study identified A-AT as a suitable adsorbent for use in the continuous removal of Cd^{2+} from aqueous solutions. The sorption of Cd^{2+} is heavily dependent on pH, ionic strength, contact time, initial metal ion concentration, and flow rate. The adsorption capacity of A-AT was 25% more than that of AT. The greatest adsorption capacity (8.83 mg/g) was obtained at a flow rate of 1 mL/min and an initial concentration of 75 mg/L. The kinetics of the adsorbent was rapid in the initial stage of the adsorption process, followed by a slow rate, and 50% of the adsorption onto the adsorbent completed within the first 3 h. The pseudo-second order adsorption kinetics model gave the best fit among the models considered for the adsorption conditions used to obtain the experimental data in the present study. The Thomas model and the Bohart-Adams model for the adsorption of Cd^{2+} onto A-AT were used to predict the adsorption mechanism under varying experimental conditions. The Bohart-Adams model gave a good fit to the experimental data. The sorption process of Cd^{2+}onto A-AT was controlled by the mass-transfer and molecular diffusion.

ACKNOWLEDGMENTS

This work was supported financially by the Natural Science Foundation of China (No. 41372233) and the Major Science and Technology Program for Water Pollution Control and Treatment (2014ZX07201-010).

REFERENCES

Aiban, S.A. (2006) Compressibility and swelling characteristics of Al-Khobar palygorskite, eastern Saudi Arabia. *Engineering Geology*, **87**, 205–219.

Aksu, Z. and Gönen, F. (2004) Biosorption of phenol by immobilized activated sludge in a continuous packed bed: prediction of breakthrough curves. *Process Biochemistry*, **39**, 599–613.

Akyuz, S., Akyuz, T., and Davies, J.E.D. (1994) Adsorption of 2,2′-bipyridyl onto sepiolite, attapulgite and smectite group clay-minerals from Anatolia – the FT-IR and FT-Raman spectra of surface and intercalated species. *Journal of Inclusion Phenomena and Molecular Recognition in Chemistry*, **18**, 123–135.

Alvarez, M., Horst, M.F., Sileo, E.E., and Rueda, E.H. (2012) Effect of Cd(II) on the ripening of ferrihydrite in alkaline media. *Clays and Clay Minerals*, **60**, 99–107.

Aly, A. and Koji, W. (1981) Adsorption of lead, copper, zinc, cobalt, and cadmium by soils that differ in cation-exchange materials. *Journal of Soil Science*, **32**, 271–283.

Bhargavi, R., Kadirvelu, K., and Kumar, N.S. (2013) Static and dynamic adsorption of phenol from aqueous solution using spherical carbon. *Carbon Materials 2012 (CCM12): Carbon Materials for Energy Harvesting, Environment, Nanoscience and Technology*, **1538**, 78–88.

Bohart, G.S. and Adams, E.Q. (1920) Some aspects of the behavior of charcoal with respect to chlorine. *Journal of the American Chemical Society*, **42**, 523–544.

Borba, C.E., da Silva, E.A., Fagundes-Klen, M.R., Kroumov, A.D., and Guirardello, R. (2008) Prediction of the copper (II) ions dynamic removal from a medium by using mathematical models with analytical solution. *Journal of Hazardous Materials*, **152**, 366–372.

Cao, C.Y., Qu, J., Wei, F., Liu, H., and Song W.G. (2012) Superb adsorption capacity and mechanism of flowerlike magnesium oxide nanostructures for lead and cadmium ions. *ACS Applied Materials & Interfaces*, **4**, 4283–4287.

Chen, H. and Wang, A.Q. (2009) Adsorption characteristics of Cu(II) from aqueous solution onto poly(acrylamide)/attapulgite composite. *Journal of Hazardous Materials*, **165**, 223–231.

Chen, J.H., Li, G.P., Liu, Q.L., Ni, J.C., Wu, W.B., and Lin, J.M. (2010) Cr(III) ionic imprinted polyvinyl alcohol/sodium alginate (PVA/SA) porous composite membranes for selective adsorption of Cr(III) ions. *Chemical Engineering Journal*, **165**, 465–473.

Chen, Z.G., Chen, F., Li, X.Z., Lu, X.W., Ni, C.Y., and Zhao, X.B. (2010) Facile synthesis of CeO_2 nanotubes templated by modified attapulgite. *Journal of Rare Earths*, **28**, 566–570.

Chowdhury, S., Chakraborty, S., and Saha, P.D. (2013) Response surface optimization of a dynamic dye adsorption process: a case study of crystal violet adsorption onto NaOH-modified rice husk. *Environmental Science and Pollution Research International*, **20**, 1698–1705.

Ding, C.L. and Shang, C.I. (2010) Mechanisms controlling adsorption of natural organic matter on surfactant-modified iron oxide-coated sand. *Water Research*, **44**, 3651–3658.

Falayi, T. and Ntuli, F. (2013) Removal of heavy metals and neutralisation of acid mine drainage with un-activated attapulgite. *Journal of Industrial and Engineering Chemistry*, **20**, 1285–1292.

Fan, H.M., He, S.H., Gu, Z.P., Zhou, Y., and Si, J.W. (2009) Adsorption of Cd^{2+} in aqueous solution by natural attapulgite. *Water Sciences and Engineering Technology*, **2**, 30–32.

Frini-Srasra, N. and Srasra, E. (2010) Acid treatment of south Tunisian palygorskite: Removal of Cd(II) from aqueous and phosphoric acid solutions. *Desalination*, **250**, 26–34.

Guerra, D.L., Silva, E.M., and Airoldi, C. (2010) Application of modified attapulgites as adsorbents for uranyl uptake from aqueous solution – thermodynamic approach. *Process Safety and Environmental Protection*, **88**, 53–61.

Haden, W.L. and Schwint, I.A. (1967) Attapulgite – its properties and applications. *Industrial and Engineering Chemistry*, **59**, 58–69.

He, Z.Y., Nie, H.L., Branford-White, C., Zhu, L.M., Zhou, Y.T., and Zheng, Y. (2008) Removal of Cu^{2+} from aqueous solution by adsorption onto a novel activated nylon-based membrane. *Bioresource Technology*, **99**, 7954–7958.

Hasan, S.H., Ranjan, D., and Talat, M. (2010) Agro-industrial waste 'wheat bran' for the biosorptive remediation of

https://doi.org/10.1346/CCMN.2014.0620505 Published online by Cambridge University Press

selenium through continuous up-flow fixed-bed column. *Journal of Hazardous Materials*, **181**, 1134–1142.

Huang, Y., Wang, H.L., and Gong, S.D. (2011) Sorption behavior of hydroxyapatite for ^{109}Cd(II) as a function of environmental conditions. *Journal of Radioanalytical and Nuclear Chemistry*, **292**, 545–553.

Inglezakis, V.J., Stylianous, M.A., Gkantzou, D., and Loizidou, M.D. (2007) Removal of Pb(II) from aqueous solutions by using clinoptilolite and bentonite as adsorbents. *Desalination*, **210**, 248–256.

John, M.K. (1972) Cadmium adsorption maxima of soils as measured by the Langmuir isotherm. *Canadian Journal of Soil Science*, **52**, 343–350.

Lian, L.L., Guo, L.P., and Guo, C.J. (2009) Adsorption of Congo red from aqueous solutions onto Ca-bentonite. *Journal of Hazardous Materials*, **161**, 126–131.

Liu, Z.N. and Liu, Y. (2014) Structure and properties of forming adsorbents prepared from different particle sizes of coal fly ash. *Chinese Journal of Chemical Engineering*, in press.

Lin, J.W., Zhan, Y.H., Zhu, Z.L., and Xing, Y.Q. (2011) Adsorption of tannic acid from aqueous solution onto surfactant-modified zeolite. *Journal of Hazardous Materials*, **193**, 102–111.

Liu, P. and Wang, T.M. (2007) Adsorption properties of hyperbranched aliphatic polyester grafted attapulgite towards heavy metal ions. *Journal of Hazardous Materials*, **149**, 75–79.

Ma, J.F., Cui, B.Y., Dai, J., and Li, D.L. (2011) Mechanism of adsorption of anionic dye from aqueous solutions onto organobentonite. *Journal of Hazardous Materials*, **186**, 1758–1765.

Ngah, W.S.W and Fatinathan, S. (2008) Adsorption of Cu(II) ions in aqueous solution using chitosan beads, chitosan–GLA beads and chitosan–alginate beads. *Chemical Engineering Journal*, **143**, 62–72.

Pehlivan, E., Yanik, B.H., Ahmetli, G., and Pehlivan, M. (2008) Equilibrium isotherm studies for the uptake of cadmium and lead ions onto sugar beet pulp. *Bioresource Technology*, **99**, 3520–3527.

Peng, S.C., Huang, C.H., Chen, T.H., Feng, Y.L., and Wang S.S. (2004) Study of the properties of adsorption of Cr^{3+} on attapulgite activated with hydrochloric acid. *Journal of Hefei University of Technology*, **27**, 611–614.

Pokhrel, D. and Viraraghavan, T. (2008) Arsenic removal in an iron oxide coated fungal biomass column: Analysis of breakthrough curves. *Bioresource Technology*, **99**, 2067–2071.

Pan, B.C., Meng, F.W., Chen, X.Q., Pan, B.J., Li, X.T., Zhang, W.M., Zhang, X., Chen, J.L., Zhang, Q.X., and Sun, Y. (2005) Application of an effective method in predicting breakthrough curves of fixed bed adsorption on to resin adsorbent. *Journal of Hazardous Materials*, **124**, 74–80.

Qi, Z.G., Shi, G.F., and Bai, L.M. (2007) Study on adsorption of phenol in wastewater by microwave modified attapulgite clay. *Non-Metallic Mines*, **30**, 56–59.

Saglam, H., Ozdemir, O., Celik, M.S., and EI-Shall, H. (2000) Adsorption mechanism of toxic metal ions by attapulgite. *Mineral processing on the verge of the 21st century*, 673–678.

Salehi, E., Madaeni, S.S., and Heidary, F. (2012) Dynamic adsorption of Ni(II) and Cd(II) ions from water using 8-hydroxyquinoline ligand immobilized PVDF membrane: Isotherms, thermodynamics and kinetics. *Separation and Purification Technology*, **94**, 1–8.

Singh, K.P., Gupta, S., Singh, A.K., and Sinha, S. (2011) Optimizing adsorption of crystal violet dye from water by magnetic nanocomposite using response surface modeling approach. *Journal of Hazardous Materials*, **186**, 1462–1473.

Suárez Barrios, M., Flores Gonzalez, L.V., Vicente Rodriguez, M.A., and Martin Pozas, J.M. (1995) Acid activation of a palygorskite with HCl: Development of physico-chemical, textural and surface properties. *Applied Clay Science*, **10**, 247–258.

Thomas, H.C. (1944) Heterogeneous ion exchange in a flowing system. *Journal of the American Chemical Society*, **66**, 1664–1666.

Uddin, M.T., Rukanuzzaman, M., Khan, M.M., and Islam, M.A. (2009) Adsorption of methylene blue from aqueous solution by jackfruit (*Artocarpus heteropyllus*) leaf powder: A fixed-bed column study. *Journal of Environmental Management*, **90**, 3443–3450.

Wang, X.H. and Wang, A.Q. (2010) Removal of Cd(II) from aqueous solution by a composite hydrogel based on attapulgite. *Environmental Technology*, **31**, 745–753.

Wang, X.H., Zheng, Y., and Wang, A.Q. (2009) Fast removal of copper ions from aqueous solution by chitosan-g-poly(acrylic acid)/attapulgite composites. *Journal of Hazardous Materials*, **168**, 970–977.

Wang, Y., Mu, Y., Zhao, Q.B., and Yu, H.Q. (2006) Isotherms, kinetics and thermodynamics of dye biosorption by anaerobic sludge. *Separation and Purification Technology*, **50**, 1–7.

Wu, N.M. and Zheng, K.L. (2013) Synthesis and characterization of poly(HEA MALA) hydrogel and its application in removal of heavy metal ions from water. *Chemical Engineering Journal*, **215–216**, 894–902.

Xi, Y., Mallavarapu, M., and Naidu, R. (2010) Adsorption of the herbicide 2,4-D on organo-palygorskite. *Applied Clay Science*, **49**, 255–261.

Xiao, K., Wang, X.M., Huang, X., Waite, T.D., and Wen, X. (2009) Analysis of polysaccharide, protein and humic acid retention by microfiltration membranes using Thomas' dynamic adsorption model. *Journal of Membrane Science*, **342**, 22–34.

Zhang, J.M., Peng, S., and Chen, J.J. (2012) Sorption of 2, 4-dichlorophenol in soil and comparison of partition coefficients obtained by batch and column experiments. *Chinese Journal of Environmental Engineering*, **6**, 4251–4256.

Zou, X.H., Pan, J.M., Ou, H.X., Wang, X., Guan, W., Li, C.X., Yan, Y.S., and Duan, Y.Q. (2011) Adsorptive removal of Cr(III) and Fe(III) from aqueous solution by chitosan/attapulgite composites: Equilibrium, thermodynamics and kinetics. *Chemical Engineering Journal*, **167**, 112–121.

(*Received 26 April 2014; revised 27 September 2014; Ms. 870; AE: E. Garcia Romero*)

https://doi.org/10.1346/CCMN.2014.0620505 Published online by Cambridge University Press